In situ magnetic and structural analysis of epitaxial $Ni_{80}Fe_{20}$ thin films for spin-valve heterostructures

I. Hashim and H. A. Atwater
Thomas J. Watson Laboratory of Applied Physics, California Institute of Technology, Pasadena, California 91125

We have investigated structural and magnetic properties of epitaxial (100) $Ni_{80}Fe_{20}$ films grown on relaxed Cu/Si(100) seed layers. The crystallographic texture and orientation of these films was analyzed *in situ* by reflection high energy electron diffraction (RHEED), and *ex situ* by x-ray diffraction and cross-sectional transmission electron microscopy (XTEM). In particular, RHEED intensities were recorded during epitaxial growth, and intensity profiles across Bragg rods were used to calculate the surface lattice constant, and hence the film strain. XTEM analysis indicated that the epitaxial films had atomically abrupt interfaces. The magnetic properties of these epitaxial films were measured *in situ* using magneto-optic Kerr effect magnetometry. Large H_c (10–20 Oe) was observed for epitaxial $Ni_{80}Fe_{20}$ (100) films less than 10.0 nm thick whereas for larger thicknesses, H_c decreased to a few Oe with the appearance of a uniaxial anisotropy. Correlations were made between magnetic properties of these epitaxial films and the strain in the film.

INTRODUCTION

Permalloy ($Ni_{80}Fe_{20}$) heterostructures are of great interest for magnetoresistive devices based on anomalous antiferromagnetic (AF)-coupling and giant magnetoresistance (GMR) in $Ni_{80}Fe_{20}$/Cu multilayers[1] and spin-valves.[2] To date, all investigations of such $Ni_{80}Fe_{20}$ heterostructures have employed polycrystalline films with atomically rough interfaces where the interface roughness is of the same order as the nonmagnetic spacer layer thickness.[1,2] Since AF-coupling and GMR depend sensitively on $Ni_{80}Fe_{20}$/Cu interface structure and the film morphology, the magnetotransport properties of atomically abrupt epitaxial films should more clearly elucidate the underlying physics. With atomically abrupt film interfaces, it would be possible to fabricate thinner nonmagnetic spacer layers without the interface roughness being the limiting factor.[1] Furthermore, the growth of epitaxial single layer $Ni_{80}Fe_{20}$ films on silicon would be potentially of great interest for studying magnetotransport and for applications to magnetoresistive devices because of reduced interfacial and grain-boundary scattering.[3] Finally, the growth of epitaxial magnetic films and the effects of coherency strain on magnetic properties especially anisotropy and magnetic moment have been the object of many previous investigations.[4] In particular, magnetic properties of epitaxial Fe and Ni thin films on Cu(100) have been studied recently[5,6] whereas strain relaxation in epitaxial Ni(100) films on Cu(100) has been examined in the past by Matthews and Crawford.[7] However, unlike Ni and Fe, $Ni_{80}Fe_{20}$ possesses very little magnetocrystalline anisotropy ($\sim 10^3$ ergs/cm^3) and the primary source of anisotropy is uniaxial anisotropy induced during deposition.

Epitaxial $Ni_{80}Fe_{20}$(100) films were grown on relaxed Cu(100) seed layers, 10–50 nm thick, oriented epitaxially with respect to Si(100). Because of the relatively small lattice mismatch between $Ni_{80}Fe_{20}$ and Cu (1.85%), the $Ni_{80}Fe_{20}$ layers were semicoherent with the Cu seed layer. The epitaxy of Cu(100) at room temperature on H-terminated Si(100) has been the object of earlier investigations and has been successfully demonstrated to occur in high-vacuum and UHV conditions.[8–10] The crystallographic orientation for this epitaxy was found to be Cu(100) ‖ Si(100) with Cu[100] ‖ Si[110].[10] Furthermore, FeMn, which is typically used in spin valves to exchange bias one of the ferromagnetic layers,[2] has an epitaxial relationship with $Ni_{80}Fe_{20}$. Hence, epitaxial spin-valve heterostructures consisting of FeMn/$Ni_{80}Fe_{20}$/Cu/$Ni_{80}Fe_{20}$ were grown on Cu/Si(100). The magnetotransport properties of these heterostructures will be reported elsewhere.[12]

EXPERIMENTAL PROCEDURES

The basic elements of the sputtering system used for deposition, x-ray diffraction analysis, electron microscopy, magneto-optic Kerr effect (MOKE) system for magnetic *in situ* characterization, and RHEED measurements to determine the surface lattice constant and the strain in the films, are described elsewhere.[10,11] In particular, $Ni_{80}Fe_{20}$ films were deposited in the presence of an external magnetic field to induce a uniaxial anisotropy.[13]

EPITAXIAL STRAIN AND MAGNETIC PROPERTIES

For growth of an overlayer B on substrate A and for small misfit f ($\leqslant$10%) between lattice constants for A and B, the lattice of B may expand or contract to form a coherent interface with that of A. However, formation of such an interface is associated with a strain energy in the overlayer B. For large enough thicknesses, it becomes energetically more favorable to relieve this coherency strain energy by generation of misfit dislocations at the interface. The critical epitaxial thickness h_c for which this transition takes place is obtained by solving the transcendental equation:[14]

$$h_c = \frac{b}{8\pi f \cos\alpha}\left[\frac{1-\nu\cos^2\beta}{1+\nu}\right]\ln\left(\frac{4h_c}{b}\right), \tag{1}$$

where b is the misfit dislocation Burger's vector, ν is the Poisson's ratio, β and α are the angles that the Burger's vector makes with the dislocation line and the direction normal to the dislocation line lying within the plane of the in-

 0021-8979/94/75(10)/6516/3/$6.00

terface, respectively. Substituting the lattice constant of $Ni_{80}Fe_{20}$ for b, $\alpha=\beta=60°$ which is often the case for fcc crystals, ν of 0.31 for Ni and misfit f for $Ni_{80}Fe_{20}$/Cu, h_c was found to be 4.1 nm from solving Eq. (1). With the onset of misfit dislocations above the critical thickness, the elastic strain in the film decreases as given by:[14]

$$\epsilon_{\parallel}=\frac{b^2}{8\pi h\cos\alpha}\left[\frac{1-\nu\cos^2\beta}{1+\nu}\right]\ln\left(\frac{4h_c}{b}\right). \tag{2}$$

As the above equation indicates, the elastic strain falls off approximately inversely with thickness h of the film. Thus, residual strain may persist in the film for thicknesses much larger than the critical thickness h_c.

Among the effects of coherency strain on magnetic properties, it has been well known that a perpendicular anisotropy can be induced in ultrathin films due to interaction with strain.[15] Furthermore, coherency strain can give rise to a biaxial in-plane stress which can couple to magnetic anisotropy via magnetostriction λ_{ij} of the thin film. However, it is well know that for Ni-Fe composition of 81% and 19%, respectively, the magnetostriction of NiFe thin films is near zero and isotropic, but nevertheless, still sensitive to the exact composition and texture of the film.[16]

Using linear elasticity theory, the in-plane stress due to coherency strain along ⟨100⟩ cubic axes in a coherent thin film can be expressed in terms of the elastic constants c_{ij} and the in-plane strain $\epsilon_{\parallel}$:[17]

$$\sigma_{\parallel}=\left[(c_{11}+c_{12})-\frac{2c_{12}^2}{c_{11}}\right]\epsilon_{\parallel}. \tag{3}$$

Substituting the elastic constants for Ni and the misfit f for $\epsilon_{\parallel}$, and λ for $Ni_{80}Fe_{20}$ (100)-textured films obtained from that reported by Klokholm and Aboaf,[16] $\sigma_{\parallel}$ was calculated using Eq. (3) and substituted in:

$$E_{me}=\tfrac{3}{2}\lambda\sigma\sin^2\theta \tag{4}$$

to estimate magnetoelastic energy E_{me} of $\sim 10^5$ ergs/cm^3 where θ is the angle between σ and the magnetization vector. This can be compared with the induced uniaxial anisotropy energy E_k for $Ni_{80}Fe_{20}$ which is typically $\sim 10^3$–10^4 ergs/cm^3. The fact that magnetoelastic energy associated with coherency strain is significantly higher than uniaxial anisotropy energy, suggests that for coherent films of $Ni_{80}Fe_{20}$, the former would be an important factor in governing magnetic anisotropy.

RESULTS AND DISCUSSION

Surface lattice constant measurements using RHEED shown in Fig. 1, were employed to observe the relaxation of the coherency strain in $Ni_{80}Fe_{20}$ films on Cu/Si(100). Due to the relatively small mismatch between Cu and $Ni_{80}Fe_{20}$ (1.85%) and the limited resolution of the camera used for recording RHEED images, it was difficult to accurately calculate the strain in the $Ni_{80}Fe_{20}$ film using this technique. Nevertheless, it can be observed from these studies that the $Ni_{80}Fe_{20}$ film relaxes to its bulk lattice constant after 4.5 nm.

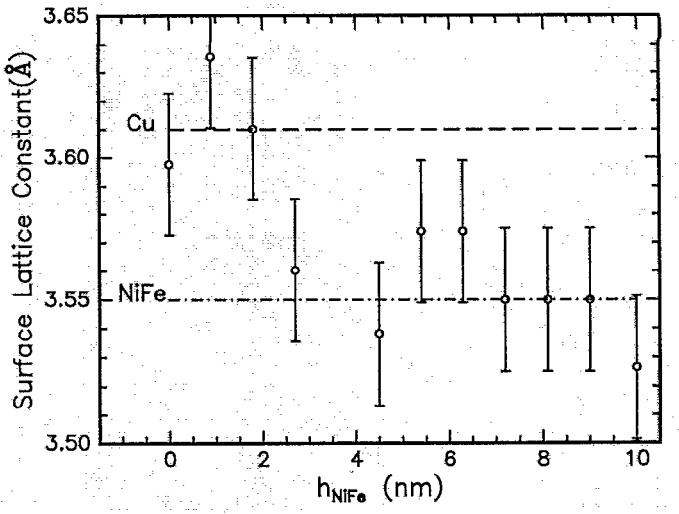

FIG. 1. Surface lattice constants as calculated from RHEED measurements of (100) $Ni_{80}Fe_{20}$ film grown on Cu/Si(100) as a function of film thickness.

No change in the RHEED intensity profiles was observed during epitaxial growth of $Ni_{80}Fe_{20}$ on Cu suggesting a layer-by-layer growth mechanism.

Figure 2 shows an x-ray scan for $\theta_i=30°$ for a $Ni_{80}Fe_{20}$ (30 nm)/Cu(30 nm)/Si(100) film which indicates that the (100) texture in the films is 2–3 orders of magnitude stronger than other fcc textures, notably (111). Furthermore, the lattice constants calculated from the diffraction spectrum confirm that the Cu and the $Ni_{80}Fe_{20}$ films are strain-relieved; i.e., have the bulk lattice constants.

Figure 3 shows a high resolution cross-sectional transmission electron micrograph of an epitaxial $Ni_{80}Fe_{20}$(50 nm)/Cu(50 nm)/Si(100) film along [110] Si in which metal lattice fringes can be seen extending from the Cu/Si interface to $Ni_{80}Fe_{20}$ film surface. The inset shows the selected area diffraction pattern due to (100) $Ni_{80}Fe_{20}$/Cu films and the Si substrate. The $Ni_{80}Fe_{20}$/Cu interface cannot be clearly seen in Fig. 3 due to lack of Z-contrast between $Ni_{80}Fe_{20}$ and Cu. However, it is discernible by the presence of Moiré fringes and misfit dislocations indicating a semicoherent interface between Cu and $Ni_{80}Fe_{20}$. Furthermore, a mosiac spread of

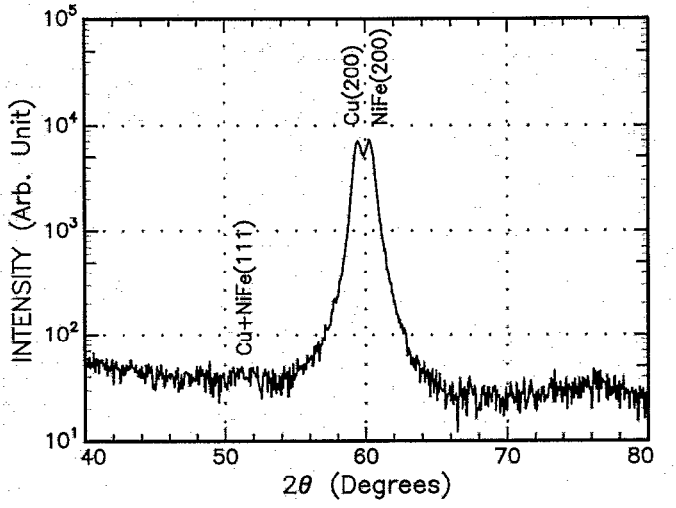

FIG. 2. Co K_α x-ray diffraction spectrum of epitaxial (100) $Ni_{80}Fe_{20}$(30 nm)/ Cu(30 nm)/Si(100).

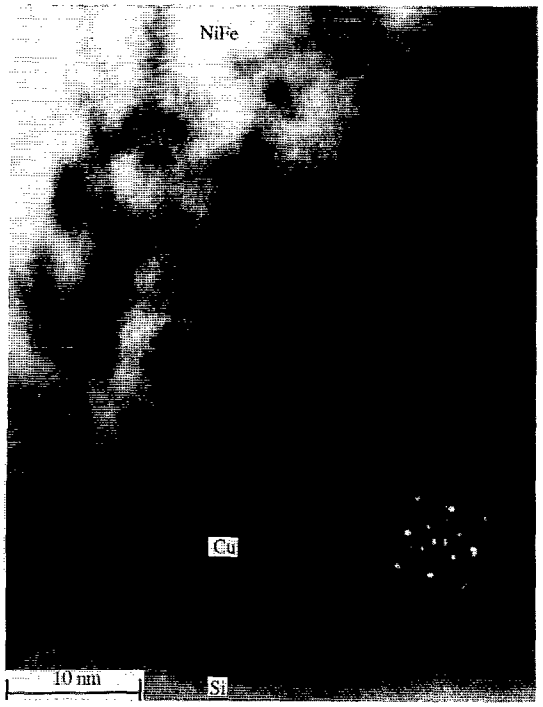

FIG. 3. High resolution cross-sectional transmission electron micrograph of epitaxial $Ni_{80}Fe_{20}$/Cu/Si(100) film along the Si[110] zone axis. The inset shows the diffraction pattern due to the film and the Si substrate.

up to $\pm 6^\circ$ in the (100) texture can be observed in the lattice fringes as well as the diffraction pattern due to the film. The smooth $Ni_{80}Fe_{20}$ film surface and the atomically abrupt Cu/Si interface suggest that the r.m.s. roughness of the epitaxial $Ni_{80}Fe_{20}$/Cu interface is few atomic layers. However, interdiffusion of Ni or Fe into Cu or vice-versa cannot be ruled out.

Magnetic properties of the epitaxial $Ni_{80}Fe_{20}$/Cu films, 2.0–20.0 nm thick, were measured using MOKE magnetometry. No MOKE signal could be detected for $Ni_{80}Fe_{20}$ films less than 2.0 nm thick. For films with thicknesses $\leq$10.0 nm, a biaxial anisotropy of ~10 Oe along the [100] crystallographic directions of $Ni_{80}Fe_{20}$ was observed which could be due to interaction with coherency strain as discussed earlier and/or magnetocrystalline anisotropy of $Ni_{80}Fe_{20}$. The coercivity for these films was 10–20 Oe which is rather high for $Ni_{80}Fe_{20}$. For random polycrystalline films deposited under the same conditions on SiO_2/Si, it was 1–2 Oe; see Fig. 4 for variation of H_c with film thickness for $Ni_{80}Fe_{20}$ films grown on Cu/Si and SiO_2/Si. Thicker epitaxial $Ni_{80}Fe_{20}$ films ($\geq$ 10.0 nm) had an induced uniaxial anisotropy due to the external magnetic field applied during deposition. Furthermore, these films had relatively soft magnetic properties (H_{ce}=2.04 Oe, H_{ch}=0.22 Oe, and H_k=12.3 Oe) which were comparable to those of random polycrystalline $Ni_{80}Fe_{20}$ films. This indicates that these films are relatively strain-free and devoid of defects or pinning sites for domain walls. It is

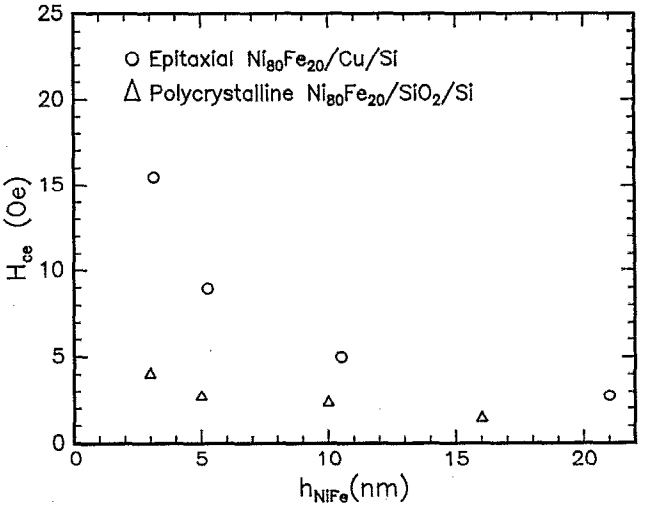

FIG. 4. Variation of H_c with $Ni_{80}Fe_{20}$ film thickness for epitaxial films on Cu/Si and polycrystalline films on SiO_2/Si.

plausible that the thinner epitaxial films have voids or sources of localized stresses due to coherency strain, which cause domain wall pinning and hence, higher H_c. Investigations are currently under way to identify the nature of these defects using atomic force microscopy.

ACKNOWLEDGMENTS

This work was supported by NSF and IBM. We would also like to acknowledge DOE grant DEFGO589ER75511 which made the use of Inel Thin Film Diffractometer possible for x-ray analysis. We thank Kirill Shcheglov and Wurzel Keir for assistance with MOKE software and hardware development, Carol Garland for assistance with electron microscopy, Bruce Gurney for helpful advice in the design of the MOKE magnetometer, and Byungwoo Park and Hyun Song Joo for help with various parts of this project.

[1] S. S. P. Parkin, Appl. Phys. Lett. **60**, 512 (1992).
[2] B. Dieny, V. S. Speriosu, B. A. Gurney, S. S. P. Parkin, D. R. Wilhoit, K. P. Roche, S. Metin, D. T. Peterson, and S. Nadimi, J. Magn. Magn. Mater. **93**, 101 (1991).
[3] A. F. Mayadas and M. Shatzkes, Phys. Rev. B **1**, 1382 (1970).
[4] R. F. C. Farrow, S. S. P. Parkin, and V. S. Speriosu, J. Appl. Phys. **64**, 5315 (1988).
[5] L. R. Sill, M. B. Brodsky, S. Bowen, and H. C. Hamaker, J. Appl. Phys. **57**, 3663 (1985).
[6] G. Bochi, C. A. Ballentine, H. E. Inglefield, S. S. Bogomolov, C. V. Thompson, and R. C. O'Handley, Mater. Res. Soc. Proc. Vol. 313, (1993).
[7] J. W. Matthews and J. L. Crawford, Thin Solid Films **5**, 187 (1970).
[8] C. A. Chang, Appl. Phys. Lett. **55**, 2754 (1989).
[9] J. Li and Y. Shacham-Diamand, J. Electrochem. Soc. **139**, L37 (1992).
[10] I. Hashim, B. Park, and H. A. Atwater, Appl. Phys. Lett. **63**, 2833 (1993).
[11] I. Hashim and H. A. Atwater, Mater. Res. Soc. Proc. Vol. 313, (1993).
[12] H. S. Joo, I. Hashim, and H. A. Atwater (unpublished).
[13] M. Takahashi, J. Appl. Phys. **33**, 1101 (1962).
[14] J. W. Matthews and A. E. Blakeslee, J. Cryst. Growth. **27**, 118 (1974).
[15] J. G. Gay and Roy Richter, Phys. Rev. Lett. **56**, 2278 (1986).
[16] E. Klokholm and J. A. Aboaf, J. Appl. Phys. **52**, 2474 (1981).
[17] J. Y. Tsao, *Materials Fundamentals of Molecular Beam Epitaxy* (Academic, San Diego, 1993), p. 106.